

Experimental observation of the spin Hall effect of light on a nano-metal film via weak measurements

Xinxing Zhou, Zhicheng Xiao, Hailu Luo,* and Shuangchun Wen[†]
*Key Laboratory for Micro-/Nano-Optoelectronic Devices of Ministry of Education,
 College of Information Science and Engineering,
 Hunan University, Changsha 410082, People's Republic of China*
 (Dated: October 30, 2018)

We theorize the spin Hall effect of light (SHEL) on a nano-metal film and demonstrate it experimentally via weak measurements. A general propagation model to describe the relationship between the spin-orbit coupling and the thickness of the metal film is established. It is revealed that the spin-orbit coupling in the SHEL can be effectively modulated by adjusting the thickness of the metal film, and the transverse displacement is sensitive to the thickness of metal film in certain range for horizontal polarization light. Importantly, a large negative transverse shift can be observed as a consequence of the combined contribution of the ratio and the phase difference of Fresnel coefficients.

PACS numbers: 42.25.-p, 42.79.-e, 41.20.Jb

I. INTRODUCTION

The spin Hall effect of light (SHEL) manifests itself as the split of a linearly polarized beam into left- and right-circular components when a beam propagates through homogeneous media. The splitting in the SHEL, governed by the angular momentum conservation law [1, 2], takes place as a result of an effective spin-orbit coupling. The SHEL is sometimes referred to as the Imbert-Fedorov effect, which was theoretically predicted by Fedorov and experimentally confirmed by Imbert [3, 4]. Generally the transverse shift of the SHEL is on the subwavelength scale, and it is difficult to be directly measured with the conventional experimental methods. In 2008, benefiting from the weak measurement technique, Hosten and Kwiat first measured the transverse displacement of refracted light [5]. The SHEL has been widely investigated in different physical systems, such as high-energy physics [6, 7], plasmonics [8–10], optical physics [11–16], and semiconductor physics [17, 18].

The SHEL holds great potential applications, such as manipulating electron spin states and precision metrology [5]. The SHEL itself may become a useful metrological tool for characterizing the refractive index variations of nanostructure. Thus, the relationship between SHEL and nanostructure is important, yet it is not fully understood. To measure the refractive index variations at subwavelength scale, we need to establish the relationship between the SHEL and the structural parameters of the nanostructure. It is well known that the SHEL manifests itself as the spin-orbit coupling. Now a question arises: What role does the structural parameters of the subwavelength nanostructure play in the spin-orbit coupling?

In this work, we establish a general propagation model

to describe the SHEL on the nano-metal film and reveal the impact of the structural parameters on the SHEL. We find that the spin-orbit coupling in the SHEL can be effectively modulated by adjusting the thickness of the metal film. It should be noted that the interesting SHEL on this structure is different from that on pure glass prism [5, 15], metal bulk [19], and layered nanostructure [20]. The paper is organized as follows. First, we analyze the SHEL on the nano-metal film theoretically. Our findings indicate that the transverse displacement of the SHEL is sensitive to the thickness of the metal film and undergoes a large negative value for horizontal polarization. Next, we focus our attention on the experiment (weak measurements). Here, the sample is a BK7 substrate coated with a thin Ag film. The experimental results are in good agreement with the theory. Finally, a conclusion is given in the fourth section.

II. THEORETICAL MODEL

Figure 1 schematically illustrates the SHEL of beam reflection on a nano-metal film in Cartesian coordinate system. The z axis of the laboratory Cartesian frame (x, y, z) is normal to the interface of the metal film at $z = 0$. The incident and reflected electric fields are presented in coordinate frames (x_i, y_i, z_i) and (x_r, y_r, z_r) , respectively. In the spin basis set, the angular spectrum can be written as $\tilde{\mathbf{E}}_i^H = (\tilde{\mathbf{E}}_{i+} + \tilde{\mathbf{E}}_{i-})/\sqrt{2}$ and $\tilde{\mathbf{E}}_i^V = i(\tilde{\mathbf{E}}_{i-} - \tilde{\mathbf{E}}_{i+})/\sqrt{2}$. Here, H and V represent horizontal and vertical polarizations, respectively. The positive and negative signs denote the left- and right-circularly polarized (spin) components, respectively.

The incident monochromatic Gaussian beam can be formulated as a localized wave packet whose spectrum is arbitrarily narrow, and can be written as

$$\tilde{\mathbf{E}}_{i\pm} = (\mathbf{e}_{ix} + i\sigma\mathbf{e}_{iy}) \frac{w_0}{\sqrt{2\pi}} \exp\left[-\frac{w_0^2(k_{ix}^2 + k_{iy}^2)}{4}\right], \quad (1)$$

*Electronic address: hailuluo@hnu.edu.cn

[†]Electronic address: scwen@hnu.edu.cn

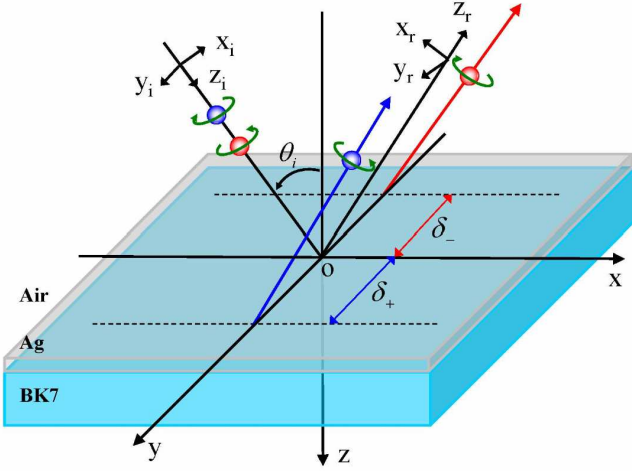


FIG. 1: (Color online) Schematic of SHEL on a nano-metal film. A linearly polarized beam reflects on the model composed of air, Ag film and the BK7 glass substrate and then splits into left- and right-circularly polarized light, respectively. δ_+ and δ_- indicate the transverse shift of left- and right-circularly polarized components. Here, θ_i is the incident angle and the Goos-Hänchen shift is not considered.

where w_0 is the beam waist. The polarization operator $\sigma = \pm 1$ corresponds to left- and right-circularly polarized light, respectively. According to the transversality, we can obtain the reflected field [20]

$$\begin{bmatrix} \tilde{\mathbf{E}}_r^H \\ \tilde{\mathbf{E}}_r^V \end{bmatrix} = \begin{bmatrix} r_p & \frac{k_{ry} \cot \theta_i (r_p + r_s)}{k_0} \\ -\frac{k_{ry} \cot \theta_i (r_p + r_s)}{k_0} & r_s \end{bmatrix} \begin{bmatrix} \tilde{\mathbf{E}}_i^H \\ \tilde{\mathbf{E}}_i^V \end{bmatrix}. \quad (2)$$

Here, r_p and r_s denote Fresnel reflection coefficients for parallel and perpendicular polarizations, respectively. k_0 is the wave number in free space.

From Eqs. (1) and (2), we can obtain the expressions of the reflected angular spectrum

$$\tilde{\mathbf{E}}_r^H = \frac{r_p}{\sqrt{2}} \left[\exp(+ik_{ry}\delta_r^H) \tilde{\mathbf{E}}_{r+} + \exp(-ik_{ry}\delta_r^H) \tilde{\mathbf{E}}_{r-} \right], \quad (3)$$

$$\tilde{\mathbf{E}}_r^V = \frac{ir_s}{\sqrt{2}} \left[-\exp(+ik_{ry}\delta_r^V) \tilde{\mathbf{E}}_{r+} + \exp(-ik_{ry}\delta_r^V) \tilde{\mathbf{E}}_{r-} \right]. \quad (4)$$

Here, $\delta_r^H = (1 + r_s/r_p) \cot \theta_i / k_0$, $\delta_r^V = (1 + r_p/r_s) \cot \theta_i / k_0$, and $\tilde{\mathbf{E}}_{r\pm}$ can be written as

$$\tilde{\mathbf{E}}_{r\pm} = (\mathbf{e}_{rx} + i\sigma\mathbf{e}_{ry}) \frac{w_0}{\sqrt{2\pi}} \exp \left[-\frac{w_0^2(k_{rx}^2 + k_{ry}^2)}{4} \right]. \quad (5)$$

It is known that the spin-orbit coupling is the intrinsic physical mechanism of the SHEL. We note that, in Eqs. (3) and (4), the terms $\exp(\pm ik_{ry}\delta_r^H)$ and $\exp(\pm ik_{ry}\delta_r^V)$ indicate the spin-orbit coupling terms in the case of horizontal and vertical polarizations [5]. The

spin-orbit coupling terms stem from the transverse nature of the photon polarization: The polarizations associated with the plane-wave components undergo different rotations in order to satisfy the transversality after reflection [5]. We can find that increasing or decreasing term $\delta_r^{H,V}$ will significantly enhance or suppress the spin-orbit coupling effect.

It is noted that the real parts of the spin-orbit coupling terms $\delta_r^{H,V}$ denote the spatial shift of the SHEL [21]. Hence, we can obtain the initial transverse displacement of the SHEL on the nano-metal film:

$$\delta_{\pm}^H = \mp \frac{\lambda}{2\pi} \left[1 + \frac{|r_s|}{|r_p|} \cos(\varphi_s - \varphi_p) \right] \cot \theta_i, \quad (6)$$

$$\delta_{\pm}^V = \mp \frac{\lambda}{2\pi} \left[1 + \frac{|r_p|}{|r_s|} \cos(\varphi_p - \varphi_s) \right] \cot \theta_i, \quad (7)$$

where $r_{p,s} = |r_{p,s}| \exp(i\varphi_{p,s})$ and λ is wavelength of the incident beam. Calculating the reflected shifts of the SHEL requires the explicit solution of the boundary conditions at the interfaces. Thus, we need to know the generalized Fresnel reflection of the metal film,

$$r_A = \frac{R_A + R'_A \exp(2ik_0 \sqrt{\varepsilon - \sin^2 \theta_i} d)}{1 + R_A R'_A \exp(2ik_0 \sqrt{\varepsilon - \sin^2 \theta_i} d)}. \quad (8)$$

Here, $A \in \{p, s\}$, R_A and R'_A is the Fresnel reflection coefficients at the first interface and second interface, respectively. ε and d represent the permittivity and thickness of the metal film, respectively.

To obtain a clear physical picture, we plot Fig. 2 to reveal what role the thickness of the nano-meta film plays in the spin-orbital coupling. Figure 2(a) and 2(b) show the initial transverse shifts of the SHEL with different film thickness. In the case of horizontal polarization, we find that the transverse displacement is extremely sensitive to the thickness when it is less than about 10nm. We find that this interesting phenomenon is attributed to the large variations of $|r_s|/|r_p|$ [Fig. 2(c)]. However, as for vertical polarizations, the transverse shift is insensitive to the thickness because of small variations of $|r_p|/|r_s|$ [Fig. 2(d)]. It should be noted that, from Eqs. (3) and (6), the term of $|r_s|/|r_p|$ plays a dominant role in spin-orbit coupling. Hence, we can enhance or suppress the SHEL effectively by modulating the thickness of the metal film. Similar effect can also be observed in a layered nanostructures, in which the transverse displacement changes periodically with the air gap increasing or decreasing due to the optical Fabry-Perot resonance [20].

In the case of horizontal polarization, the transverse shift experiences large negative value [Fig. 2(a)], which is different from the SHEL on a metal bulk [19]. From Eqs. (6) and (7), we can find that, for a fixed incident angle, negative shifts entail the combined contributions of the large ratio of Fresnel coefficients ($|r_s|/|r_p|$ or $|r_p|/|r_s|$) and phase difference induced negative $\cos(\varphi_s - \varphi_p)$ or $\cos(\varphi_p - \varphi_s)$ [Fig. 2(e) and 2(f)] which are due to the material properties of the metal film. We conclude that

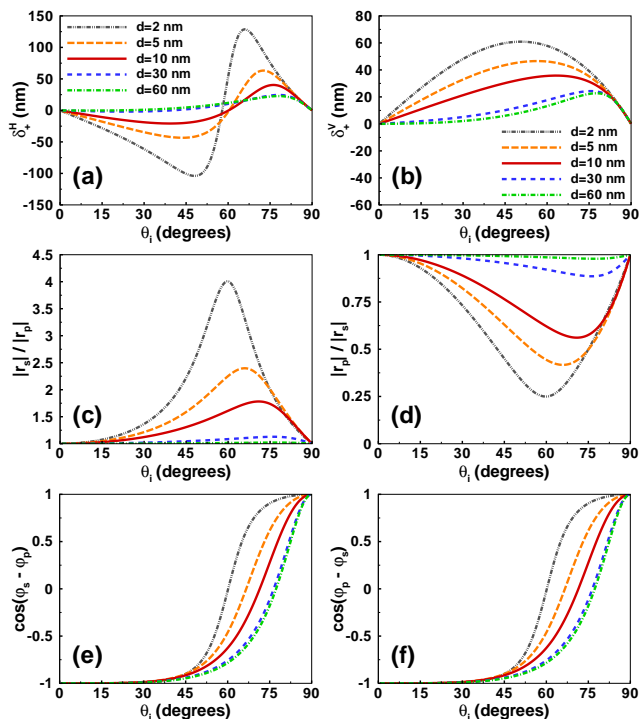


FIG. 2: (Color online) Role of the thickness of nano-meta film in the SHEL. (a) and (b) represent the transverse displacements of the SHEL on the thin Ag film under the condition of horizontal and vertical polarization. We choose the thickness of the thin metal film from 2 to 60nm. (c) and (d) show the value of $|r_s|/|r_p|$ and $|r_p|/|r_s|$. (e) and (f) denote the value of $\cos(\varphi_s - \varphi_p)$ and $\cos(\varphi_p - \varphi_s)$ for the different thickness. Here, the permittivity of Ag is chosen as $\varepsilon = -18 + 0.5i$ and the refractive index of the BK7 substrate is chosen as $n = 1.515$ at 632.8nm.

large negative transverse displacement only exists in the case of horizontal polarization while always is positive under the condition of vertical polarizations. It is indicated that by rotating the polarization of incident light beam, we are able to switch the direction of the spin accumulation [22] effectively. Similar phenomena also occur in electronic system. Here, the spin accumulation can be switched by altering the directions of an external magnetic field [23–25]. By rotating the polarization plane of the exciting light, the directions of spin current can be switched in a semiconductor microcavity due to the spin Hall effect [26, 27].

III. EXPERIMENTAL OBSERVATION

To detect the tiny transverse shifts, we use the signal enhancement technique known as the weak measurements [28, 29]. Note that the weak measurements has attracted a lot of attention and holds great promise for precision metrology [30–35]. The theoretical analysis of the SHEL on nano-metal film has yielded two major results: sensitive SHEL in extremely thin metal film and

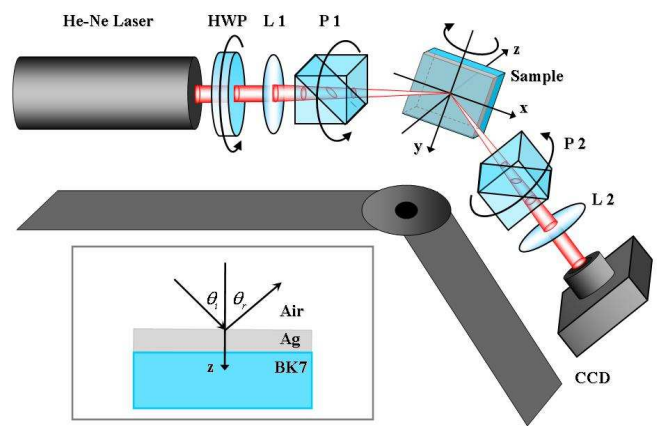


FIG. 3: (Color online) Experimental setup: Sample, a BK7 glass substrate coated with Ag film. L1 and L2, lenses with effective focal length 50mm and 250mm, respectively. HWP, half-wave plate (for adjusting the intensity). P1 and P2, Glan Laser polarizers. CCD, charge-coupled device (Coherent LaserCam HR). The light source is a 17mW linearly polarized He-Ne laser at 632.8nm (Thorlabs HRP170). The inset shows the detailed information about the sample. Here, the dark shadow represents the optical rail.

large negative beam shift of horizontal polarized incident beam. However, we inevitably face a major obstacle that prevents us from experimentally corroborating the first claim because fabricating Ag film thinner than 10nm would unavoidably involve large technical errors. Nonetheless, we still attempt to verify the validity of our theory by measuring the SHEL in large film thickness. In this section, we choose the BK7 glass substrate coated Ag film as our sample (with three different thickness 10nm, 30nm and 60nm).

Our experimental setup shown in Fig. 3 is similar to that in Refs [5, 15]. A Gauss beam generated by a He-Ne laser firstly impinges onto the HWP which is used to control the light intensity to prevent the charge-coupled device (CCD) from saturation. And then, the light beam passes through a short focal length lens (L1) and a polarizer (P1) to produce an initially linearly polarized focused beam. When the beam reaches the sample interface, the SHEL takes place. The sample is a BK7 glass substrate coated with a thin Ag film whose permittivity is $\varepsilon = -18 + 0.5i$ at 632.8nm [36]. As the reflected beam splits by a fraction of the wavelength, the two components interfere destructively after the second polarizer (P2), which is oblique to P1 with an angle of $90^\circ \pm \Delta$. In our weak measurements experiment, we choose the angle $\Delta = 0.4^\circ$. Then we use L2 to collimate the beam and make the beam shifts insensitive to the distance between L2 and the CCD. Finally, we use a CCD to measure the amplified shift after L2. It should be mentioned that the amplified factor A_w is not a constant, which verifies the similar result of our previous work [22].

We measure the displacements of the SHEL on the nano-metal film every 5° from 30° to 85° in the case of horizontal and vertical polarization, respectively. Lim-

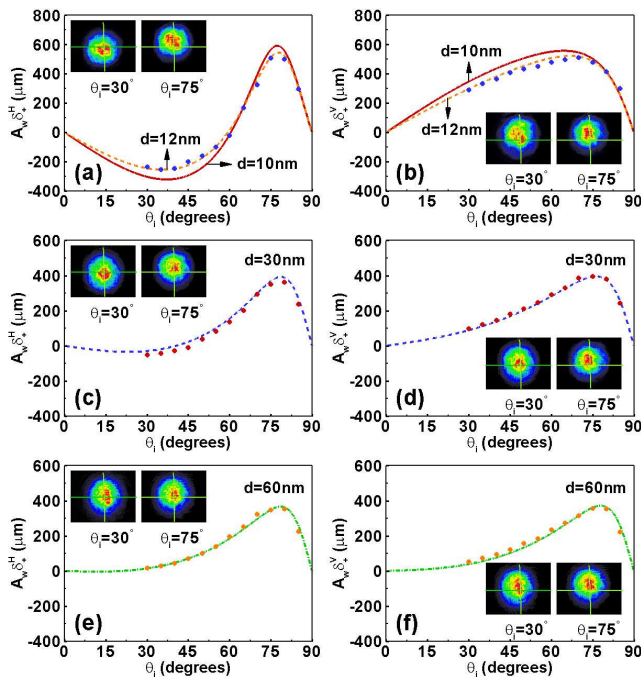


FIG. 4: (Color online) The amplified displacements of horizontal polarized (left column) and vertical polarized (right column) beam reflection on Ag film with different thicknesses: [(a),(b)] 10nm and 12nm, [(c),(d)] 30nm, and [(e),(f)] 60nm. A_w represents the amplified factor of the weak measurements. The lines indicate the theoretical value and the dots show the experimental results (the error ranges are less than $10\mu\text{m}$). The insets show the measured field distributions from the CCD.

ited by the large holders of the lens, polarizers and He-Ne laser, displacements at small incident angles were not measured. Figure 4 plots the amplified displacement in both theoretically and experimentally. In the case of horizontal polarization, the shift first experiences a negative value and then increases with the incident angle. After reaching the peak value in the incident angle about 75° , the shift decreases rapidly. For three different thicknesses, the negative shifts are vary. With the thickness increasing, the range of negative shift decreases. In the case of vertical polarization, the shift first increases with the incident angle and also decreases rapidly after the

peak value. But, there exists no negative values compared with the horizontal polarization.

It should be noted that the experimental results are in good agreement with the theoretical ones when the film thicknesses are 30nm and 60nm [Fig. 4(c)-(f)]. However, we observe a small deviation when the thickness is 10nm [Fig. 4(a) and 4(b)]. Note that the thickness of the nano-metal film has an error in the range of $\pm 5\text{nm}$, limited by the experimental condition. When the thickness reaches to 10nm, the SHEL is very sensitive to the error. It is the reason why there is a small deviation between the experimental and the theoretical data. From the experimental results, we can conclude that the actual thickness of the film is about 12nm. This interesting characteristic may provide a potential way for measuring the thickness of the nano-metal film.

IV. CONCLUSIONS

In conclusion, we have observed the SHEL on a nano-metal film experimentally via weak measurements. We have found that the spin-orbit coupling effect can be effectively manipulated by adjusting the thickness of the metal film. Our findings indicate that the transverse displacement is sensitive to the thickness of the metal film in certain range. Hence, altering the metal film thickness will enhance or suppress the SHEL significantly. As an analogy of spin Hall effect in an electronic system, we are able to switch the directions of the spin accumulation in SHEL effectively by rotating the polarization of incident light beam. These findings provide a pathway for modulating the SHEL and thereby open the possibility of developing nanophotonic applications.

Acknowledgments

One of the authors (X. Z.) thanks Dr. Y. Qin and Dr. N. Hermosa for helpful discussions. We are sincerely grateful to the anonymous referee, whose comments have led to a significant improvement on our paper. This research was supported by the National Natural Science Foundation of China (Grants Nos. 61025024, 11074068).

[1] M. Onoda, S. Murakami, and N. Nagaosa, Phys. Rev. Lett. **93**, 083901 (2004).
 [2] K. Y. Bliokh and Y. P. Bliokh, Phys. Rev. Lett. **96**, 073903 (2006).
 [3] F. I. Fedorov, Dokl. Akad. Nauk SSSR **105**, 465 (1955).
 [4] C. Imbert, Phys. Rev. D **5**, 787 (1972).
 [5] O. Hosten and P. Kwiat, Science **319**, 787 (2008).
 [6] P. Gosselin, A. Bérard, and H. Mohrbach, Phys. Rev. D **75**, 084035 (2007).
 [7] C. A. Dartora, G. G. Cabrera, K. Z. Nobrega, V. F. Montagner, M. H. K. Matielli, F. K. R. de Campos, and H.

T. S. Filho, Phys. Rev. A **83**, 012110 (2011).
 [8] Y. Gorodetski, A. Niv, V. Kleiner, and E. Hasman, Phys. Rev. Lett. **101**, 043903 (2008).
 [9] K. Y. Bliokh, Y. Gorodetski, V. Kleiner, and E. Hasman, Phys. Rev. Lett. **101**, 030404 (2008).
 [10] L. T. Vuong, A. J. L. Adam, J. M. Brok, P. C. M. Planken, and H. P. Urbach, Phys. Rev. Lett. **104**, 083903 (2010).
 [11] K. Y. Bliokh, A. Niv, V. Kleiner, and E. Hasman, Nature Photon. **2**, 748 (2008).
 [12] A. Aiello and J. P. Woerdman, Opt. Lett. **33**, 1437

- (2008).
- [13] D. Haefner, S. Sukhov, and A. Dogariu, *Phys. Rev. Lett.* **102**, 123903 (2009).
- [14] O. G. Rodríguez-Herrera, D. Lara, K. Y. Bliokh, E. A. Ostrovskaya, and C. Dainty, *Phys. Rev. Lett.* **104**, 253601 (2010).
- [15] Y. Qin, Y. Li, H. He, and Q. Gong, *Opt. Lett.* **34**, 2551 (2009).
- [16] H. Luo, S. Wen, W. Shu, Z. Tang, Y. Zou, and D. Fan, *Phys. Rev. A* **80**, 043810 (2009).
- [17] J.-M. Ménard, A. E. Mattacchione, M. Betz, and H. M. van Driel, *Opt. Lett.* **34**, 2312 (2009).
- [18] J.-M. Ménard, A. E. Mattacchione, H. M. van Driel, C. Hautmann, and M. Betz, *Phys. Rev. B* **82**, 045303 (2010).
- [19] N. Hermosa, A. M. Nugrowati, A. Aiello and J. P. Woerdman, *Opt. Lett.* **36**, 3200 (2011).
- [20] H. Luo, X. Ling, X. Zhou, W. Shu, S. Wen, and D. Fan, *Phys. Rev. A* **84**, 033801 (2011).
- [21] A. Aiello, M. Merano, and J. P. Woerdman, *Phys. Rev. A* **80**, 061801 (2009).
- [22] H. Luo, X. Zhou, W. Shu, S. Wen, and D. Fan, *Phys. Rev. A* **84**, 043806 (2011).
- [23] J. Sinova, D. Culcer, Q. Niu, N. A. Sinitsyn, T. Jungwirth, and A. H. MacDonald, *Phys. Rev. Lett.* **92**, 126603 (2004).
- [24] T. Kimura, Y. Otani, T. Sato, S. Takahashi, and S. Maekawa, *Phys. Rev. Lett.* **98**, 156601 (2007).
- [25] G. Mihály, M. Csontos, S. Bordács, I. Kézsmarki, T. Wojtowicz, X. Liu, B. Jankó, and J. K. Furdyna, *Phys. Rev. Lett.* **100**, 107201 (2008).
- [26] A. Kavokin, G. Malpuech, and M. Glazov, *Phys. Rev. Lett.* **95**, 136601 (2005).
- [27] C. Leyder, M. Romanelli, J. Ph. Karr, E. Giacobino, T. C. H. Liew, M. M. Glazov, A. V. Kavokin, G. Malpuech, and A. Bramati, *Nature Phys.* **3**, 628 (2007).
- [28] Y. Aharonov, D. Z. Albert, and L. Vaidman, *Phys. Rev. Lett.* **60**, 1351 (1988).
- [29] N. W. M. Ritchie, J. G. Story, and R. G. Hulet, *Phys. Rev. Lett.* **66**, 1107 (1991).
- [30] G. J. Pryde, J. L. O'Brien, A. G. White, T. C. Ralph, and H. M. Wiseman, *Phys. Rev. Lett.* **94**, 220405 (2005).
- [31] P. B. Dixon, D. J. Starling, A. N. Jordan, and J. C. Howell, *Phys. Rev. Lett.* **102**, 173601 (2009).
- [32] N. Brunner, and C. Simon, *Phys. Rev. Lett.* **105**, 010405 (2010).
- [33] S. Kocsis, B. Braverman, S. Ravets, M. J. Stevens, R. P. Mirin, L. K. Shalm, and A. M. Steinberg, *Science* **332**, 1170 (2011).
- [34] A. Feizpour, X. X. Xing, and A. M. Steinberg, *Phys. Rev. Lett.* **107**, 133603 (2011).
- [35] O. Zilberberg, A. Romito, and Y. Gefen, *Phys. Rev. Lett.* **106**, 080405 (2011).
- [36] E. D. Palik, *Handbook of Optical Constants of Solids* (Academic, New York, 1998).